This article has been accepted for publication in a future issue of this journal, but has not been fully edited. Content may change prior to final publication. Citation information: DOI 10.1109/TAP.2018.2820322, IEEE Transactions on Antennas and Propagation

Electromagnetic Modeling of Self-tuning RFID Sensor Antennas in Linear and Nonlinear Regimes

M. C. Caccami and G. Marrocco, *IEEE Member*

***Abstract*—Multi-state chips for UHF Radiofrequency Identification ensure self-compensation of the variations in antenna impedance. This self-tuning capability can provide a digital information about the change in local boundary conditions within the vicinity of the tag. This feature can be exploited further for low-cost wireless sensing applications.**

An electromagnetic model of the tag in linear and nonlinear regimes allows prediction of analog and digital response of the device depending on the boundary conditions that cause the variation of the antenna impedance and/or gain. Additionally, the model provides estimation of the degradation in communication performance of the tag due to imperfect retuning of the chip impedance. The theoretical findings of the model are verified in sensing applications using a reference self-tuning tag. Sensing measurements of liquid compounds in linear regime and of the water-filling level of a box in nonlinear regime are demonstrated as a practical application of the proposed mathematical model.

***Index Terms*—RFID sensing, Wireless sensors, Internet of Things, Self-tuning tags.**

I. Introduction[1]

In recent years, the widescale adoption of the UHF Radiofrequency Identification (RFID) technology [1] has boosted the multi-face evolution of the Internet of Things [2]-[4]. In addition to the traditional applications in logistics, potential of passive RFID tags for sensing of physical parameters are widely investigated [5]. The two main architectures comprises of *i*) tags with sensor-oriented chips that digitalize the sensed data at the chip level so that the reader receives a digital data that is rather immune to the propagation noise, and *ii)* tags with standard chips where the antenna itself plays the role of transducer between the physical signal and the amplitude or the phase of the modulated backscattered electromagnetic field [6] - [8]. While the first class is suitable for medium-cost ($>$ \$ 10) accurate sensing in industrial infrastructures, the latter could, instead, be useful for low-cost ($<$ \$ 1) qualitative sensing in large scale applications. The major critical issues with low-cost RFID sensors are: *i)* the sensing capabilities are often achieved at the expense of the communication performance (read distance) and *ii)* the relationship between the measured signal and the physical parameter under test (such as temperature, humidity, deformation, motion, and gases) is fully exploited at the reader side. The data readout is accordingly affected by several parameters such as propagation noise, specific arrangement of the measurement set-up, and the variation in environmental conditions [9]. The limitations of low-cost RFID sensors, related to the propagation channel and to the undesired background scattering, can be partly removed [10] by a combined post-processing of power signals related to both the forward and reverse RFID links, yielding the Analog Identifier (AID). The current limitation of this approach is its narrow dynamic range. A different idea, discussed in [11], concerns a single-port antenna provided with a multi-state impedance load so that more data are available to drop out the communication uncertainty.

In this direction, recently introduced new family of low-cost self-tuning RFID chips [12], [13] exploits the concept of dynamic input impedance. Such a chip is capable of automatic modification of its internal impedance within a discrete set. This facilitates antenna impedance to be balanced automatically in relation to the changing boundary conditions while maintaining stability in the performance of the readout. These self-tuning chips offer advantage of chip-level digitalisation of the changes in input impedance of the antenna in relation to the variations of external physical parameters. The digitized data remains un-susceptible to the propagation uncertainties. These features can be exploited for low-cost wireless sensing applications. In this regard, so far few qualitative examples of applications have been reported in literature, mostly being application notes from chip manufacturers [14]. Information about quantitative studies and suitable theoretical electromagnetic model is still lacking. Since the sensing feature of this class of devices is related to the close interactions between the antenna and the chip responses to variable boundary conditions, electromagnetic modelling is fundamental to yield a complete understanding of its functionality. Moreover, the theoretical modeling can allow mastering the response of the sensor as well as communication performance.

Following the embryonic ideas in [15], this work introduces a theoretical framework (Section II) useful to express the linear and even the nonlinear response of such self-tuning tags. This is achieved by combining the numerically evaluated response of the antenna portion with the discrete response of the self-tuning chip, thus deriving two possible sensing modalities. With reference to a real self-tuning tag (whose parameters are identified in Section III), the theoretical achievements are validated by means of two experimental test-cases involving the tag loaded with drops of different liquids (Section IV) and the same antenna used to sense the water-filling level of a box (Section V).

[1]Paper submitted on June 12, 2017, reviewed on September 1, 2017 and November 25, 2017 and resubmitted on December, 28 2017; accepted on March 16, 2018. The authors are with the Pervasive Electromagnetics Lab, www.pervasive.ing.uniroma2.it, upon the University of Roma Tor Vergata, Italy. E-mail: gaetano.marrocco@uniroma2.it, caccami@ing.uniroma2.it.

0018-926X (c) 2018 IEEE. Personal use is permitted, but republication/redistribution requires IEEE permission. See http://www.ieee.org/publications_standards/publications/rights/index.html for more information.

This article has been accepted for publication in a future issue of this journal, but has not been fully edited. Content may change prior to final publication. Citation information: DOI 10.1109/TAP.2018.2820322, IEEE Transactions on Antennas and Propagation

II. Mathematical representation of RFID sensing by self-tuning chips

A UHF RFID tag is electromagnetically characterised by the gain G_T and the admittance[2] ($Y_T = 1/Z_T = g_T + jB_T$) of its antenna and by the radiofrequency input admittance ($Y_C = 1/Z_C = g_C + jB_C$) and sensitivity p_C of the microchip radio that is connected onboard. In battery-less tags, the microchip is normally lifeless until it is turned on by an impinging field, coming from a reader unit. The power $P_{R\to T}$ delivered to the microchip transponder is given by the Friis formula under free-space conditions and a perfect impedance matching at the transmitter side:

$$P_{R\to T} = \left(\frac{\lambda}{4\pi d}\right)^2 P_{in} G_R G_T \tau \eta_p \tag{1}$$

where G_R is the gain of the reader's antenna, P_{in} is the input power feeding the reader's antenna, and d is the reader-tag distance. η_P is the tag-reader polarization efficiency and $\tau = \frac{4R_C R_T}{|Z_C+Z_T|^2} \leq 1$ is the power transfer coefficient [16] (R_C and R_T being the input resistance of the chip and of the antenna, respectively), which accounts for the impedance mismatch between the antenna and the chip. A more suitable representation for the modeling of self-tuning tags involves the admittance instead of the impedance. By enforcing the substitutions $Z_{C,T} = 1/Y_{C,T}$ and $R_{C,T} = g_{C,T}/\left|Y_{C,T}\right|^2$ it is easy to show that

$$\tau = \frac{4\frac{g_C}{|Y_C|^2}\cdot\frac{g_T}{|Y_T|^2}}{\left|\frac{1}{Y_C}+\frac{1}{Y_T}\right|^2} = \frac{4g_C g_T}{\left|Y_C+Y_T\right|^2} \leq 1 \tag{2}$$

with $\tau = 1$ if $Y_T = Y_C^*$. The tag will activate when the received power exceeds the sensitivity of the chip ($P_{R\to T} \geq p_C$).

The minimum input power, P_{in}, delivered by the reader transmitter to its antenna to collect the backscattering response from a tag placed at a distance d is denoted as turn-on power $P_{in}^{to}(d)$ [6] that can be derived from (1) by enforcing that the power delivered to the chip equals its power sensitivity, i.e. that $P_{R\to T} = p_C$.

The above electromagnetic parameters are affected by the electromagnetic interaction of the tag's antenna with the local boundary conditions such as the proximity of dielectric or metallic media. In case of conventional static-impedance microchips, an alteration of the local environment may provoke an impedance mismatch between the antenna and the microchip and a change in the tag's gain with the consequence of the read range degradation. Analog sensing capabilities [6] of the variation of some local environmental parameters (hereafter denoted as $\Psi(t)$), such as temperature [17], deformations [18], humidity [19], and presence of different gases [20]) can be exploited by a UHF RFID tag having engineered the antenna response and primarily the admittance-stimuli $Y_T \leftrightarrow \Psi$ and the gain-stimuli $G_T \leftrightarrow \Psi$ relationships. The tag's antenna itself is hence used as a transducer, possibly conditioned by a lumped or distributed chemical/mechanical sensor that is integrated onboard. Thus, a self-tuning microchip provides a means to digitise the analog sensor response at the tag level and, under some conditions, it preserves the communication performance.

[2]Small caps notation is used for the conductance with the purpose to differentiate it from the antenna gain.

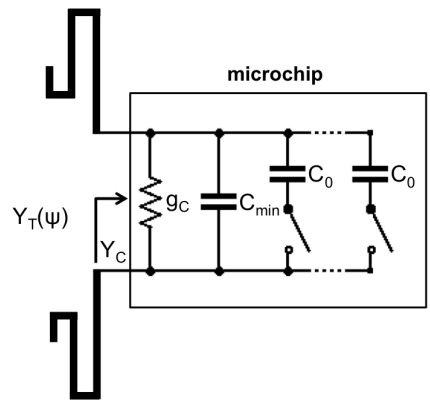

Fig. 1. Equivalent circuit of a self-tuning sensor tag.

A. Linear Regime

A typical architecture of *self-tuning* microchips (already implemented in commercial products [12], [13]) includes an adaptive internal network (Fig. 1), generally made of capacitors, whose overall capacitance is

$$C_C(n) = C_{min} + nC_0 \tag{3}$$

with C_{min} the baseline of the network and C_0 the incremental step. The instantaneous value of the tuning network is automatically adjusted by an internal logic for the purpose of maximising the power that the tag's antenna delivers to the microchip for that specific boundary condition. Accordingly, the equivalent susceptance $B_C(n) = \omega C_C(n)$ of the microchip compensates the possible deviation of the tag's admittance from the perfect matching condition, so that:

$$|B_C(n) + B_T(\Psi)| = 0. \tag{4}$$

The integer parameter $0 \leq n(\Psi) \leq N$, hereafter referred to as *sensor code,* provides an indication of the retuning effort of the chip. Accordingly, the antenna susceptance that will be perfectly compensated for by the chip has to fall within the range of

$$-\omega C_{min} - NC_0 \leq B_T \leq -\omega C_{min} \tag{5}$$

where N depends on the implementation of the chip. For the activation of the retuning, the antenna must be designed to

0018-926X (c) 2018 IEEE. Personal use is permitted, but republication/redistribution requires IEEE permission. See http://www.ieee.org/publications_standards/publications/rights/index.html for more information.

This article has been accepted for publication in a future issue of this journal, but has not been fully edited. Content may change prior to final publication. Citation information: DOI 10.1109/TAP.2018.2820322, IEEE Transactions on Antennas and Propagation

provide a negative susceptance. Moreover, values of B_T that are smaller or higher than the boundaries set in Eq. (5) will hence return saturated sensor codes to $n = N$ and $n = 0$, respectively.

Under the above hypothesis, the sensor code can be considered as an indirect measure of the admittance mismatch between the antenna and the chip in reaction to the change in the physical parameter $\Psi(t)$. Digital sensing capabilities may therefore be achieved by exploiting the sensor code as a sensing metric for the phenomenon under observation. The susceptance of the antenna $B_T(\Psi)$ plays the role of a transducer between the phenomenon Ψ and the sensor code *n* through the mapping

$$n(\Psi) = nint\left(-\frac{1}{C_0}(C_{min} + \frac{B_T(\Psi)}{\omega})\right) \tag{6}$$

where "*nint*" indicates nearest integer or round function such that $nint(x)$ is the integer number closest to x. Since the antenna's susceptance is frequency dependent, the sensor code will be moreover variable as $n(\Psi, \omega)$. It is worth noticing that values of $B_T(\Psi)$ outside the range in (5) will not provide any sensing information and Eq. (6) cannot be applied.

Under the hypothesis of perfect compensation, such that $B_C(n) = -B_T(\Psi)$, the turn-on power, evaluated at a fixed distance d_0 from the reader unit, can be written as:

$$P_{in}^{to}(d_0, \Psi) = \left(\frac{4\pi d_0}{\lambda}\right)^2 \frac{p_C}{\eta_p G_R G_T(\Psi)} \frac{(g_T(\Psi) + g_C)^2}{4 g_C g_T(\Psi)}. \tag{7}$$

This power is independent of the susceptance, while it is only affected by conductance and gain of the antenna and thus by its variation with reference to the external stimuli. Moreover, the turn-on power is directly related to the maximum read distance estimated as $d_{max} = d_0\sqrt{P_{in}^{max}/P_{in}^{to}}$, with P_{in}^{max} the maximum power the reader can provide to its antenna with. Let Ψ_0 now denote a reference condition of the phenomenon under observation for which the antenna impedance is made to perfectly match the chip, i.e. $Y_T(\Psi_0) = Y_C^*$ such that $\tau(\Psi_0) = 1$. The variation of the read distance along the evolution of the external process will be

$$\frac{d_{max}(\Psi)}{d_{max}(\Psi_0)} = \frac{2\sqrt{g_C g_T(\Psi)}}{g_T(\Psi) + g_C}\sqrt{\frac{G_T(\Psi)}{G_T(\Psi_0)}}. \tag{8}$$

Hence, the degradation of the performance in the communication is hence due to the sensitivity of both the gain and the conductance of the tag to the physical stimulus $\Psi(t)$. Therefore, the most appropriate way to apply this kind of tag as a digital sensor is to integrate a transduction mechanism onboard the antenna that produces changes only in the antenna susceptance during the variation of the external phenomenon under test, while keeping its conductance and gain unaltered. An example is an inclusion of a lumped capacitive device, like a humidity sensor [21] - [23] (with admittance $Y_S(\Psi) = g_S + j\omega C_S(\Psi)$), which is interconnected in parallel between the antenna port and the chip. Concerning the antenna, it was demonstrated in [24] that the change in the gain of a tag in presence of external humidity (i.e., following the deposition of water molecules over its metallic surface) is rather modest. It could be moreover further reduced by a proper coating of the antenna except for the lumped humidity sensor. The effective admittance of the tag will therefore be $Y_T^{'} = g_T + g_S + j(B_T + \omega C_S(\Psi))$. Accordingly, the application of the self-tuning equation (4) would enforce $|\omega C_C(n) + B_T + \omega C_S(\Psi)| = 0$ and the read distance in (8) would remain stable as $\sqrt{g_C g_T}/(g_T + g_C)$ is now independent of Ψ.

Equation (7) can be also discussed in a different way. Assume that the tag interacts with two time-variant external phenomena, say $\Psi(t)$ and $\Upsilon(t)$, which independently affect the tag susceptance $B_T(\Psi)$ and the tag conductance/gain $\{g_T(\Upsilon), G_T(\Upsilon)\}$, the self-tuning tag will, therefore, be sensitive to both the variations through the sensor code $n \leftrightarrow B_T \leftrightarrow \Psi$ and through the turn-on power $P_{in}^{to} \leftrightarrow \Upsilon$ metrics.

B. Nonlinear regime

A more general expression of the sensor code can be derived by accounting for the nonlinear behavior of RFID microchips. In fact, the RF input parameters exhibit some dependence on the strength of the impinging power [25] - [28]. In particular, due to a voltage limiter at the front-end of the IC, the equivalent RF admittance Y_C is related in a nonlinear way to the induced open-circuit voltage V_T at the antenna's terminals [1], [29]. Such voltage ([10], formulas (4 - 5)) can be written as:

$$V_T = -j\frac{\lambda}{\pi}\frac{e^{-jk_0 d}}{d}\sqrt{\frac{P_{in} G_R R_T G_T \chi}{2}} e^{j\Phi} \tag{9}$$

with k_0 being the propagation constant and $\{\chi, \Phi\}$ the polarization-dependent parameters such that $\chi = |\hat{\underline{h}}_T \cdot \hat{\underline{h}}_R|^2$ and $\Phi = angle(\hat{\underline{h}}_T \cdot \hat{\underline{h}}_R)$ with $\hat{\underline{h}}_R$ and $\hat{\underline{h}}_T$ being the effective length of the reader and tag antennas, respectively. The nonlinear effect, which is chip-family dependent, arises when the open-circuit voltage exceeds a given cut-off value ($V_T > V_{T,cutoff}$), i.e when the power delivered to the chip is much greater than the chip sensitivity ($P_{R\to T} \gg p_C$). The microchip admittance $Y_C[V_T]$ is hence a function, as per Eq. (9), of the electromagnetic parameters of the RFID link. For the specific case of self-tuning microchips, for the sake of notational simplicity, we assume that the nonlinear variation of the microchip admittance will only impact the baseline capacitance C_{min}, so that

$$C_{min} = C_{min,0} + \Delta C[V_T] \tag{10}$$

where $C_{min,0}$ is the nominal value (at the turn-on condition) and $\Delta C[V_T]$ is a distortion factor. Accordingly, by plugging (10) into (6), it is easily shown that the activation of the network reconfiguration will return the following sensor code

0018-926X (c) 2018 IEEE. Personal use is permitted, but republication/redistribution requires IEEE permission. See http://www.ieee.org/publications_standards/publications/rights/index.html for more information.

This article has been accepted for publication in a future issue of this journal, but has not been fully edited. Content may change prior to final publication. Citation information: DOI 10.1109/TAP.2018.2820322, IEEE Transactions on Antennas and Propagation

$$n(\Psi) = n_0(\Psi) - nint\left(\frac{\Delta C[V_T]}{C_0}\right) \tag{11}$$

where $n_0(\Psi)$ refers to linear regime as in (6).

The second term in (11) is then linearly approximated as

$$nint\left(\frac{\Delta C(V_T)}{C_0}\right) \approx -m\,(V_T - V_{T,\,cutoff}) \tag{12}$$

with "*m*" the nonlinearity parameter depending on the chip. Equation (11) then becomes:

$$n(\Psi) = nint\left(-\frac{1}{C_0}(C_{min,0} + \frac{B_T(\Psi)}{\omega})\right) +$$

$$+\varepsilon_v m\,(V_T(\Psi) - V_{T,\,cutoff}) \tag{13}$$

where

$$\varepsilon_v = \begin{cases} 0 \;\; if\; V_T \leq V_{T,cutoff} & \text{linear regime} \\ 1 \;\; if\; V_T > V_{T,cutoff} & \text{nonlinear regime.} \end{cases} \tag{14}$$

Therefore, from equations (9), (11), and (12), the sensor code will be in general sensitive to additional parameters other than to the pure variation of the antenna susceptance. In particular, the returned sensor code will be determined by the measurement set-up (i.e., the mutual distance and orientation between reader and tag and the power emitted by the reader) but even by the antenna gain and by its input resistance. This behavior can be turned into a different sensing modality allowing detection of the variations in the parameter under test even in absence of a true variation of the susceptance of the antenna or of the admittance ($\frac{\partial}{\partial t}Y_T(\Psi(t)) = 0$). In this case, if the chip worked in linear regime, no sensor code variation would be returned ($\frac{\partial}{\partial t}n_0(\Psi(t)) = 0$). Nevertheless, provided that the antenna gain was affected by the variation of the physical parameter under test ($\frac{\partial}{\partial t}G_T(\Psi(t)) \neq 0$), the open-circuit voltage could exceed the cut-off value ($V_T[G_T(\Psi)] > V_{T,cutoff}$) so that the chip will be forced to work in a nonlinear regime. Accordingly, the chip baseline capacitance $C_{min}[V_T]$ will deviate from the nominal value and the tag will experience a chip-antenna impedance mismatch $Y_C[V_T] \neq Y_T^*$. As a result, the self-tuning network gets activated thus returning a sensor code that is correlated to the phenomenon under observation. Examples of the described interrogation modalities will be given in the next experimental Sections.

It is worth noting that the nonlinear behavior (i.e the parameters $\{V_{T,cutoff},\, m\}$) is a peculiarity of the chip itself and does not directly depend on the antenna portion of the tag which instead determines the open-circuit voltage. The foregoing derived nonlinearity parameters are thus of general validity even if the gain and/or the input resistance of the antenna were modified by variable boundary conditions. The nonlinearity parameters can therefore be estimated in a simple reference configuration, such as an antenna in an open air, as it will be described later in Section IV. The sensor code corresponding to a particular boundary condition will then be computed by applying the mapping of $\{R_T,\, G_T\} \rightarrow V_T$ through (9) and (13), as shown in Section V.

III. A Reference Self-tuning Tag

A useful architecture to exploit the above theoretical considerations, by means of both numerical simulations and laboratory experimentations, is the SMARTRAC Sensor Dogbone [14] inlay. The tag is made of a paper substrate and is coated by a polyethylene layer (Fig. 2). The self-tuning chip is the RFMicron Magnus V.2 [12]. The tag also includes an interdigitated region, close to the chip, to magnify the sensitivity of the antenna impedance to the variation of nearby permittivity. According to the manufacturer, the chip is capable of adjusting its internal tuning capacitance in the range of $1.9 \leq C_C \leq 2.9\,pF$, while the nominal conductance is roughly fixed to $g_C = 4.38 \times 10^{-4}\,S$. The sensor code spans in the range of $0 < n < 31$. From (3) the nominal network capacitances are estimated to be $C_{min} = 1.9\,pF$ and $C_0 = 1\,pF/31$. The foregoing data are referred to the North American band (902 - 928 MHz).

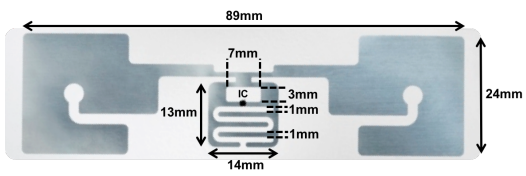

Fig. 2. SMARTRAC Sensor Dogbone integrating a self-tuning RFMicron Magnus chip and an interdigitated region.

The sensor code response of such a tag was experimentally measured by a set-up comprising a typical long-range UHF fixed reader (*ThingMagic* M6e, [30]) with $0.5\,dBm$ power resolution, connected to a linearly-polarized $5\,dB$ gain patch antenna placed at a fixed or variable distance from the sensor (as specified case by case).

The two preparatory experiments, described below, allowed us to qualify the stability of the sensor code in static conditions. Moreover, we will show how to extract the nonlinearity parameters to be used in the modelling of the experimental cases of the next Sections.

A. Dispersion of the Sensor Code

Figure 3 illustrates the sensor code versus the frequency, collected in the linear regime, i.e. when the reader operates in *power-adaptive mode*. The power emitted by the reader is gradually increased and automatically adjusted, frequency by frequency, until the tag starts responding. Accordingly, the power collected by the chip equals the microchip sensitivity p_C and the chip is forced to work just above the turn-on power for any values of the boundary conditions. The tag was placed onto a foam holder, within a partially anechoic environment, in order to approximate a free-space condition.

0018-926X (c) 2018 IEEE. Personal use is permitted, but republication/redistribution requires IEEE permission. See http://www.ieee.org/publications_standards/publications/rights/index.html for more information.

This article has been accepted for publication in a future issue of this journal, but has not been fully edited. Content may change prior to final publication. Citation information: DOI 10.1109/TAP.2018.2820322, IEEE Transactions on Antennas and Propagation

The tag was interrogated by the reader's antenna from different mutual distances ($28cm < d < 100cm$) and orientations ($\vartheta = \{-60°, -30°, 0°, 30°, 60°\}$). This configuration is denoted as *static* as the boundary condition is stationary ($\frac{\partial}{\partial t}\Psi(t) = 0$). However, on observing the tag response in a broad frequency range, the corresponding natural variation of the antenna's impedance versus the frequency will activate the self-tuning action of the chip and the returned sensor code will be accordingly frequency-dependent. The superposition of the measured sensor codes, corresponding to several reader-tag mutual configurations, gives an indication of the systematic error of the device. In particular, the sensor codes are rather stable and mostly independent of the measurement set-up, with a maximum dispersion $D_n = \max_f \{n_{max}(f) - n_{min}(f)\} = 1$, which is hence masked by the intrinsic sensor code resolution.

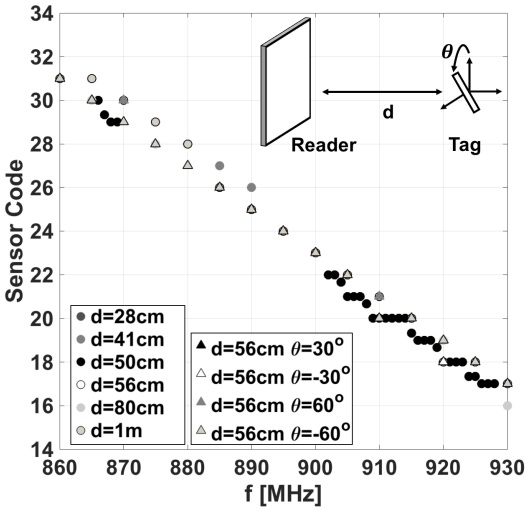

Fig. 3. Measured sensor codes collected by adaptive-power mode interrogation for different alignments and orientations between the reader's antenna and the tag (see the inset).

B. Nonlinearity parameters

The nonlinearity parameters $\{V_{T,cutoff}, m\}$ of the chip as per Eq. (12), to be used in the modelling of the tag response, can be evaluated by sourcing the reader's antenna with a gradually increasing power spanning from the turn-on value up to the allowed maximum power level $P_{in} < 31\,dBm$ by the reader. The sensor code was measured at two frequencies $f_1 = 869\,MHz$ (European) and $f_2 = 915\,MHz$ (North American). Accordingly, under the free-space condition and linear polarization between the reader's antenna and the tag, the open-circuit voltage V_T at the antenna's terminals is obtained from Eq. (9) assuming the reader-tag distance $d = 50\,cm$. The required input resistance $R_T(f)$ and gain $G_T(f)$ of the tag's antenna were obtained from simulations performed by means of the Finite Difference Time Domain (FDTD) tool (CST Microwave Studio software, [31]) having measured the antenna sizes by hand through a caliber with an approximation of roughly $0.2\,mm$. The profile of the sensor code with reference to the increasing power P_{in} emitted by the reader is shown in Fig. 4 for both considered frequencies. The open-circuit voltage at the tag antenna's terminals is thus evaluated from (9) and then superimposed in the same figure. The transition from linear to nonlinear responses clearly appears starting from the values $V_{T,cutoff}(f_1, f_2) = \{0.07,\ 0.19\}\ V$ corresponding to $n_0(f_1) = 29$ and $n_0(f_2) = 20$. By application of (11) and (12) the nonlinearity parameter *m* is estimated by linear regression

$$m(f) \approx \frac{n(f) - n_0(f)}{V_T(f) - V_{T,cutoff}(f)}. \tag{15}$$

Finally, the identification procedure returned the values $m(f_1, f_2) = \{-22.5,\ -14.7\}\ [V^{-1}]$.

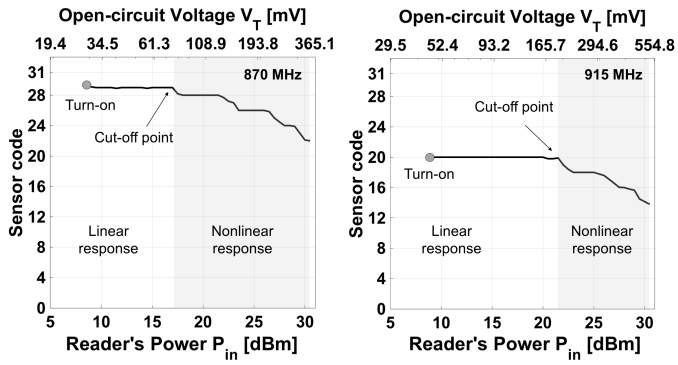

Fig. 4. Measured sensor code in air vs. reader's power and corresponding open-circuit voltage V_T at $869\,MHz$ and at $915\,MHz$.

IV. Example of Modeling of the Linear Sensing Response

The theoretical findings in Section II are here demonstrated by means of a realistic experiment of sensing through the self-tuning network. The interdigitated portion of the reference tag was loaded with drops of different liquids, having known dielectric parameters so as to allow an accurate numerical simulation.

A. Material samples

We considered a set of four liquids (Fig. 5) providing various combinations of low and high permittivity and electrical conductivity for the purpose to stimulate a broad variation of the antenna response (gain and impedance). The material denoted as *liquid phantom* is a mixture of water, sugar, and salt, resembling the human body, according to the recipe in [32]. The liquids were brought in contact with the antenna by means of a saturated absorbing paper sheet (surface area $5\ x\ 5\ mm^2$ and thickness $0.15\ mm$) placed right over the interdigitated portion, i.e. in touch with the sensing area of the tag, close to the chip. The paper substrate of the tag was removed just over that region in order to provide a direct

0018-926X (c) 2018 IEEE. Personal use is permitted, but republication/redistribution requires IEEE permission. See http://www.ieee.org/publications_standards/publications/rights/index.html for more information.

This article has been accepted for publication in a future issue of this journal, but has not been fully edited. Content may change prior to final publication. Citation information: DOI 10.1109/TAP.2018.2820322, IEEE Transactions on Antennas and Propagation

contact with the materials to be measured. Overall, the set of liquid samples can be considered as instances $\{\Psi_n\}$ of a phenomenon under observation with a broad dynamic range ($1 < \epsilon_r < 75.6$, $0 < \sigma < 1.7\, S/m$).

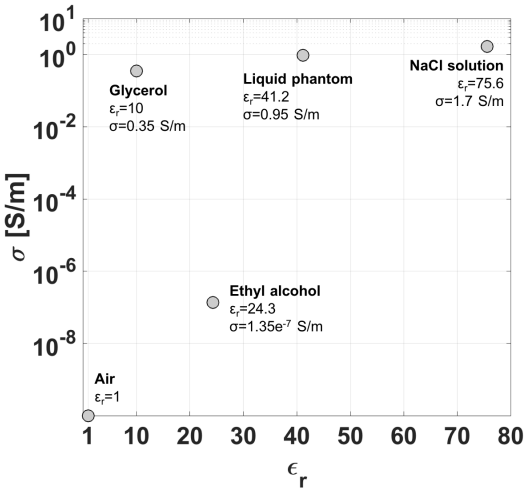

Fig. 5. Dielectric properties in the UHF RFID band of the considered liquids.

B. Numerical simulation

The interdigitated sensing portion of the tag cannot be considered as a lumped element since its size is not negligible with respect to the antenna and it is not possible to define a proper port interface. Accordingly, a full-wave numerical model of the tag as a whole was adopted to predict its electromagnetic response. The liquid samples were modelled as homogeneous thin bricks having the dielectric properties of the different materials under investigation. The input admittance of the tag $Y_T(f, \Psi_m)$ and its gain $G_T(f, \Psi_m)$ were evaluated for each liquid sample. The chip feedback was then included in post-processing by assuming a perfect compensation as in (4). The sensor code $n(f, \Psi_m)$ was finally derived through equation (6) by assuming a linear regime response. The simulated profiles of the antenna input admittance and of the antenna gain are shown in Fig. 6. The variation of the antenna susceptance to be compensated by the self-tuning chip is rather different for the considered materials. For most of them, the required tuning capacitances C_C (Fig. 7), estimated from Eq. (4), fall within the allowed range of the capacitor network except for the air in the European RFID band (865 - 868 MHz) and for the NaCl solution at the North American frequencies. The resulting mismatch of the tag in air in the EU band was expected since the tag had been designed by the manufacturer (who provided the samples) for the North American band. For the NaCl solution at the North American frequencies, the expected capacitance ($C_C(NaCl) = -B_T(NaCl)/\omega$) that the self-tuning network of the microchip should synthesize in order to match the antenna is in the range of $1.6 < C_C(NaCl) < 1.8\, pF$ and hence it is below the minimum value $C_{min} = 1.9\, pF$ of the chip. Accordingly, it is expected that the chip will fail to compensate the corresponding susceptance variation returning a sensor code that is saturated to the lowest value. Moreover, the variations of conductance and gain of the tag's antenna will produce a degradation of the read distance over the different Ψ_m, as also predicted by (8).

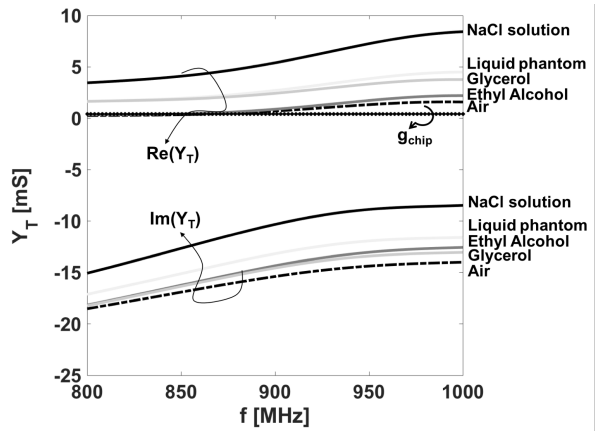

(a)

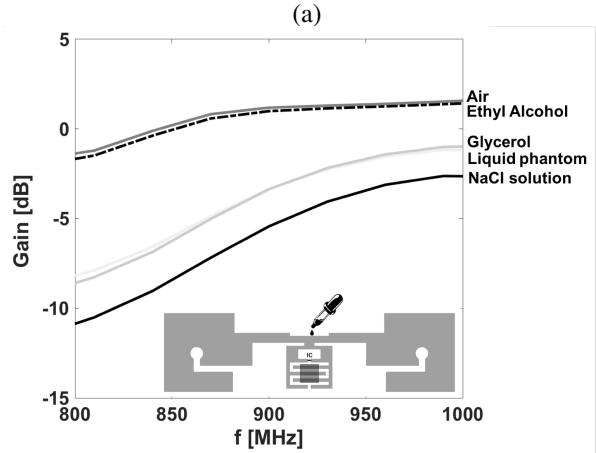

(b)

Fig. 6. Self-tuning tag loaded with different liquids: (a) simulated antenna input admittance and (b) simulated antenna gain along the antenna axis (broadside observation) versus frequency.

C. Measurements and comparisons

The measured sensor codes versus frequency, as achieved by adaptive-power mode interrogation for each considered liquid sample, as well as their numerical counterpart, are shown in Fig. 8.

A more direct comparison is instead provided in Table I at 869 and 915 MHz. In spite of some discrepancies in the European RFID band (probably due to the fact that the input parameters of the chip are available in the North America RFID band) the measured responses ($0 < n < 31$) and

0018-926X (c) 2018 IEEE. Personal use is permitted, but republication/redistribution requires IEEE permission. See http://www.ieee.org/publications_standards/publications/rights/index.html for more information.

This article has been accepted for publication in a future issue of this journal, but has not been fully edited. Content may change prior to final publication. Citation information: DOI 10.1109/TAP.2018.2820322, IEEE Transactions on Antennas and Propagation

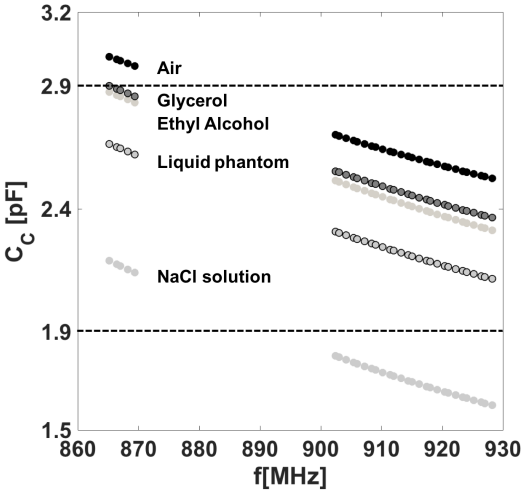

Fig. 7. Self-tuning tag loaded with different liquids: estimated values of the tuning capacitance of the chip. The horizontal lines indicate the range of C_C allowed by the RFmicron Magnus™ chip.

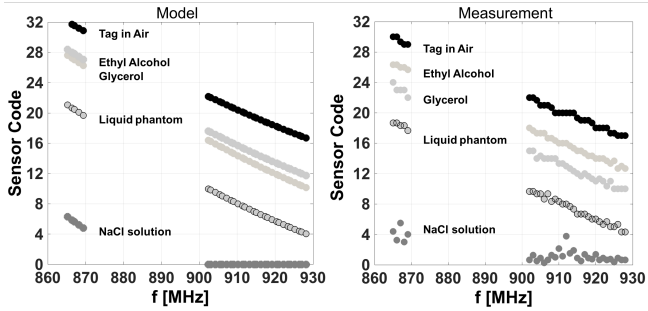

Fig. 8. Theoretical and measured sensor codes vs. frequency of the self-tuning tag whose interdigitated region was loaded with different liquid drops that were deposited onto an absorbing paper sheet.

the theoretical data are in reasonable agreement and follow comparable profiles.

TABLE I
SELF-TUNING TAG LOADED WITH DIFFERENT LIQUIDS: MEASURED AND COMPUTED SENSOR CODES AT 869 AND 915 MHz.

Liquids	Sim 869 MHz	Meas 869 MHz	Sim 915 MHz	Meas 915 MHz
Air	31	29	19	19
Ethyl Alcohol	26	26	13	15
Glycerol	27	23	14	12
Liquid phantom	20	18	7	7
NaCl solution	5	4	0	1

The experimental profiles of the turn-on power (Fig. 9(a)) show some fluctuations, especially in the North American band. They are probably due to the combined variations in the frequency of the gain and conductance of the loaded tag (as shown in Fig. 6) that the chip is unable to compensate for, as well as to the variations in frequency of the chip sensitivity and conductance that are undocumented in the datasheet. Finally, Fig. 9(b) illustrates the comparison between the estimated maximum read distances at a fixed frequency, derived from (8), when moving from the nearly lossless ethyl alcohol down to the NaCl solution having the highest electrical conductivity/permittivity. Overall, there is a good agreement between the model and measurements.

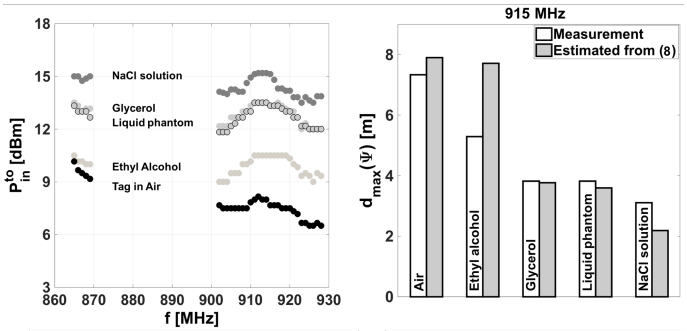

(a) (b)

Fig. 9. Self-tuning tag loaded with different liquids: (a) measured turn-on power vs. frequency and (b) comparison between measured and theoretical read distance derived from (8) at 915 MHz when the reader emits 4.0 W EIRP interrogating power.

V. EXAMPLE OF MODELING OF NONLINEAR SENSING RESPONSE

The example concerns the same tag as before, but in this case applied to the monitoring/sensing in nonlinear regime of the filling level of water inside a container. For this purpose, the tag was placed onto the external surface of a perspex cylinder (radius 2.2 cm, height 16 cm, and thickness 0.3 cm) that was gradually filled with water (see the inset in Fig. 10(b)). The simulated input admittance and the gain of the tag at 869 MHz versus the level of water are depicted in Fig. 10. The profiles of both the conductance and the susceptance are nearly constant for $2 < h < 10$ cm. The gain of the tag's antenna, instead, exhibits a major change for most of the considered range of the water level. It was verified by means of numerical simulations that this behavior is caused by the combined effect of *i*) the reshaping of the antenna directivity (following the electromagnetic interaction with a high permittivity material) and *ii*) the degradation of the radiation efficiency because of the increasing power loss into the water column. Accordingly, the open-circuit voltage $V_T(h)$ is expected, from (9), to be water level-dependent (Fig. 10(b)) following a similar profile. This parameter is computed for a reader's power value $P_{in} = 31$ $dBmW$ so that V_T will be much higher than the cut-off values of the chip ($V_{T,cutoff} = 0.07$ V). The nonlinear response of the tag will, therefore, be excited and Eq. (13) applies for $\varepsilon_v = 1$, with

0018-926X (c) 2018 IEEE. Personal use is permitted, but republication/redistribution requires IEEE permission. See http://www.ieee.org/publications_standards/publications/rights/index.html for more information.

This article has been accepted for publication in a future issue of this journal, but has not been fully edited. Content may change prior to final publication. Citation information: DOI 10.1109/TAP.2018.2820322, IEEE Transactions on Antennas and Propagation

the parameters m and $V_{T,cutoff}$ previously derived in Section III.

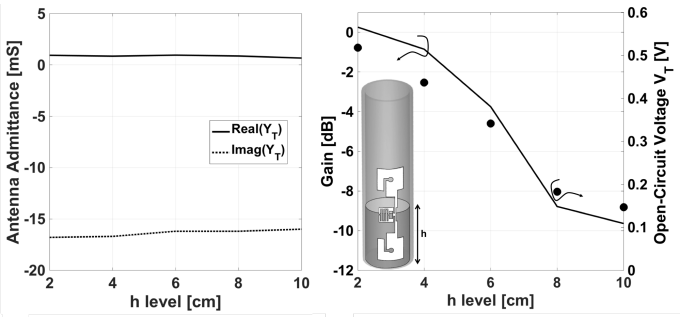

(a) (b)

Fig. 10. Box-filling experiment: the self-tuning tag senses an increasing level of water inside a perspex box where it is attached on. The reader was placed $50\,cm$ far from the pipe. (a) Simulated input admittance and (b) the antenna gain and open-circuit voltage at $869\,MHz$ versus the level of water.

The outcome of the model is in agreement with the measurements shown in (Fig. 11(a)). The sensor code profile $n(h)$ clearly reveals the possibility to detect the change in the liquid level even in the case of invariant antenna susceptance. In particular, the overall variation of the sensor code is $\Delta n = 11$ with an estimated sensitivity of the tag to the change in the water level equal to $S(h) = \frac{\Delta n}{\Delta h} = 1.1\,cm^{-1}$, as derived from the linearization of $n(h)$ profile. The system resolution, i.e. the smallest detectable variation of the quantity that is being measured, is hence $\delta h = \frac{\delta n}{S(h)} = 0.9\,cm$, where $\delta n = 1$ is the precision of the sensor code generation for the specific set-up.

Finally, for the sake of completeness, the sensor code was also measured according to an adaptive-power mode interrogation (and hence in the linear regime). As expected from the simulated nearly uniform admittance, the measured sensor code (Fig. 11(b)) is constant and saturates to its upper boundary. Hence, although the response of the antenna is altered (only concerning the gain), no information about the change in the water level is returned.

VI. Discussions and Conclusions

The paper introduced a general-purpose model of the analog and digital response of the new class of passive self-tuning RFID tag antennas in both linear and nonlinear regimes proposing two different sensing methodologies. In linear regime, i.e. when the reader operates in adaptive-power interrogation mode, the sensor code is insensitive to the mutual orientation and distance of the reader so that it looks to be a rather robust sensing indicator even in the case of a non-fixed setup, such as a hand-held reader. A fixed or at least reproducible set-up is instead required when the power emitted by the reader is kept fixed and locked to a value of emitted power that is greatly above the turn-on value so that a

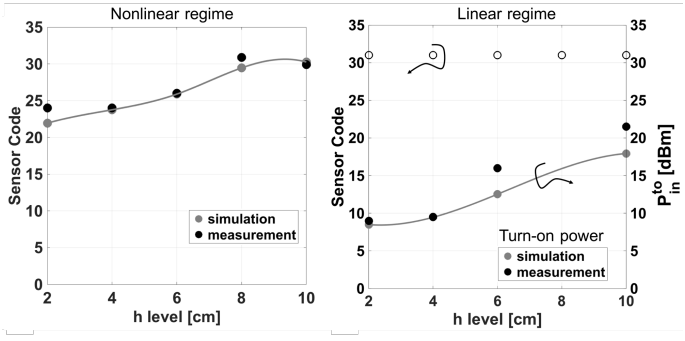

(a) (b)

Fig. 11. (a) Nonlinear regime: theoretical and measured sensor codes versus the variable water level at $869\,MHz$. (b) Linear regime: measurement of the sensor code by means of the adaptive-power mode interrogation and measured and simulated turn-on power.

nonlinear response of the microchip RF impedance is excited. Nevertheless, the fixed-power interrogation mode is capable of expanding the sensing applicability of the self-tuning chip to the cases where the phenomenon under observation does not affect the antenna admittance while instead it modifies the gain. A possible field of applications for the nonlinear sensing could be in industrial manufacturing wherein a conveyor line is involved. In this case, the tagged objects to be monitored will approach in a same reproducible way and close enough to the reader placed at a fixed and known position.

The communication performance, i.e. the maximum read distance of the tag, can be preserved along with the evolution of the physical phenomenon when an adaptive-power interrogation is exploited and only antenna susceptance is modified by $\Psi(t)$. Such a change falls right within the retuning domain of the self-tuning tag. In all the other cases, the read distance will be subjected to degradation along with $\Psi(t)$. Accordingly, the antenna response has to be properly shaped to comply with the dynamic range and resolution of the sensor. The constrained design method discussed in [33] could be, for instance, extended to this case.

In general, when compared with the state of the art of the analog RFID sensing tags [6], that only enable a qualitative monitoring [9], and with the more powerful tags with sensor-oriented chips (including an internal Analog to Digital Conversion, [34]), this class of self-tuning UHF tag antennas fall in between. Indeed, they still employ the antenna as part of the transduction mechanism but the intelligence required to extract the sensing data is now split between both the tag and the reader sides and the source of error due to the signal transmission is removed. However, the retrieved sensing content has to be considered as relative and an application-specific calibration is still required. Since their cost is expected to be comparable with that of the conventional tags for logistics, they could be suited to for large scale applications such as, for instance, foods or perishable products. The sensor

0018-926X (c) 2018 IEEE. Personal use is permitted, but republication/redistribution requires IEEE permission. See http://www.ieee.org/publications_standards/publications/rights/index.html for more information.

data may hence complement the identification of goods with some, still qualitative, information about their physical status.

VII. Acknowledgments

Work supported by the *Consolidate the Foundations - RadioSkin* project funded by the University of Rome Tor Vergata. The authors thank RFmicron and SMARTRAC for having provided samples as well as for the useful technical support and the valuable discussions.

References

[1] D. M. Dobkin, "The RF in RFID: Passive UHF RFID in Practice," Amsterdam, The Netherlands: Elvesier, 2007.

[2] L. Atzori, A. Iera, G. Morabito, "The Internet of Things: A survey," *Comput. Netw.,* vol. 54, no. 15, pp. 2787 - 2805, Oct. 2010.

[3] X. Jia, Q. Feng, T. Fan, and Q. Lei, "RFID Technology and its Applications in Internet of Things (IOT)," *Proc. of 2012 Int. Conf. on Consumer Electron. Comm. Netw. (CECnet)*, Yichang (China), Apr. 2012.

[4] L. Catarinucci, D. De Donno, L. Mainetti, L. Palano, L. Patrono, M. L. Stefanizzi, and L. Tarricone, "An IoT-Aware Architecture for Smart Healthcare Systems," *IEEE Internet Things J.,* vol. 2, no. 6, pp. 515 - 526, Dec. 2015.

[5] J. Zhang, G. Y. Tian, A. M. J. Marindra, A. I. Sunny, and A. B. Zhao, "A Review of Passive RFID Tag Antenna-Based Sensors and Systems for Structural Health Monitoring Applications," *Sensors*, vol. 2, no. 17, 265, 2017.

[6] C. Occhiuzzi, S. Caizzone and G. Marrocco, "Passive UHF RFID antennas for sensing applications: Principles, methods, and classifcations," *IEEE Antennas Propag. Mag*., vol. 55, no. 6, pp. 14 - 34, Dec. 2013.

[7] M. C. Caccami, S. Manzari and G. Marrocco, "Phase-Oriented Sensing by Means of Loaded UHF RFID Tags," *IEEE Trans. Antennas Propag.*, vol. 63, no. 10, pp. 4512 - 4520, Oct. 2015.

[8] J. Grosinger, L. Görtschacher, and W. Bösch, "Passive RFID Sensor Tag Concept and Prototype Exploiting a Full Control of Amplitude and Phase of the Tag Signal," *IEEE Trans. Microw. Theory Techn.*, vol. 64, no. 12, pp. 4752 - 4762, Dec. 2016.

[9] C. Occhiuzzi and G. Marrocco, "Precision and Accuracy in UHF-RFID Power Measurements for Passive Sensing," *IEEE Sens. J.*, vol. 16, no. 9, pp. 3091 - 3098, May 2016.

[10] G. Marrocco, "RFID Grids: Part I—Electromagnetic Theory," *IEEE Transactions on Antennas and Propagation*, vol. 59, no. 3, pp. 1019 - 1026, March 2011.

[11] S. Capdevila, L. Jofre, J. Romeu, and J. C. Bolomey, "Multi-Loaded Modulated Scatterer Technique for Sensing Applications," *IEEE Trans Instrum Meas.,* vol. 62, no. 4, pp. 794 - 805, April 2013.

[12] RFmicron Magnus™ UHF RFID Tag IC, RFID tag chip antenna design guideline, Application Note [Online]. Available: www.rfmicron.com.

[13] Monza® R6 Tag Chip Datasheet, Application Note [Online]. Available: www.impinj.com.

[14] SMARTRAC Sensor Dogbone, Application Note [Online]. Available: www.smartrac-group.com.

[15] M. C. Caccami and G. Marrocco, "Electromagnetic Characterisation of Self-Tuning UHF RFID Tags for Sensing Application," *2016 IEEE AP-S Sym. Antennas Propag. USNC-URSI Radio Sci. Meet.*, Fajardo, Puerto Rico, June 26 - July 1, 2016.

[16] C. A. Balanis, "Antenna theory: analysis and design," *Microstrip Antennas*, 3rd edition, John Wiley & Sons, 2005.

[17] A.A. Babar, S. Manzari, L. Sydanheimo, A. Z. Elsherbeni, and L. Ukkonen, "Passive UHF RFID Tag for Heat Sensing Applications," *IEEE Trans. Antennas Propag.*, vol. 60, no. 9, pp. 4056 - 4064, Sept. 2012.

[18] R. Bhattacharyya, C. Floerkemeier, and S. Sarma, "Towards tag antenna based sensing - An RFID displacement sensor," *RFID, 2009 IEEE Int. Conf.*, pp. 95 - 102, 27 - 28 April 2009.

[19] J. Virtanen, L. Ukkonen, T. Bjorninen, A. Elsherbeni, and L. Sydandnheimo, Inkjet printed humidity sensor for passive uhf rfid systems, *IEEE Trans Instrum Meas.*, vol. 60, pp. 2768 - 2777, Aug. 2011.

[20] L. K. Fiddes and N. Yan, "RFID Tags for wireless electrochemical detection of volatile chemicals," *Sens Actuators B Chem*, pp. 817 - 823, May 2013.

[21] HIH-4000. Application Note [Online]. Available: https://sensing.honeywell.com/honeywell-sensing-hih4000-series-product-sheet-009017-5-en.pdf.

[22] 818 Full range 0 - 100%RH humidity sensor. Application Note [Online]. Available: http://www.sensorelement.com/humidity/818%20humidity.pdf.

[23] H. Bi, K. Yin, X. Xie, J. Ji, S. Wan, L. Sun, M. Terrones, and M. S. Dresselhaus, "Ultrahigh humidity sensitivity of graphene oxide," *Sci Rep.,* vol. 3, no. 2714, Sept. 2013.

[24] S. Manzari, C. Occhiuzzi, S. Nawale, A. Catini, C. Di Natale, and G. Marrocco, "Humidity Sensing by Polymer-loaded UHF RFID Antennas," IEEE Sens. J., vol.12, no. 9, pp. 2851 - 2858, 2012.

[25] T. Bauernfeind, K. Preis, G. Koczka, S. Maier, and O. Biro, "Influence of the Non-Linear UHF-RFID IC Impedance on the Backscatter Abilities of a T-Match Tag Antenna Design," *IEEE Trans Magn,* vol. 48, no. 2, pp. 755 - 758, Feb. 2012.

[26] G. Andíia Vera, Y. Duroc and S. Tedjini, "Third Harmonic Exploitation in Passive UHF RFID," *IEEE Trans. Microw. Theory Techn.*, vol. 63, no. 9, pp. 2991 - 3004, Sept. 2015.

[27] Pavel V. Nikitin, K. V. S. Rao, "Harmonic scattering from passive UHF RFID tags," *2009 IEEE Antennas Propag. Soc. Int. Sym.*, Charleston, SC, 2009, pp. 1 - 4.

[28] J-M. Hannula, K. Rasilainen, V. Viikari, "Characterization of transponder antennas using intermodulation response," *IEEE Trans. Antennas Propag*., vol. 63, no. 6, pp. 2412 - 2420, June 2015.

[29] J. C. Bolomey, S. Capdevila, L. Jofre, and J. Romeu, "Electromagnetic Modeling of RFID-Modulated Scattering Mechanism. Application to Tag Performance Evaluation," *Proc. IEEE*, vol. 98, no. 9, pp. 1555 - 1569, Sept. 2010.

[30] ThingMagic M6e. [Online]. Available: http://www.thingmagic.com/index.php/fixed-rfid-readers/mercury6, accessed Jan. 2014.

[31] CST Microwave Studio Suite®, 2017. [Online]. Available: https://www.cst.com.

[32] G. Hartsgrove, A. Kraszewsky, and A. Surowiec, "Simulated biological materials for electromagnetic radiation absorption studies," *Bioelectromagnetics*, vol. 8, no. 4, pp. 29 - 36, 1987.

[33] C. Occhiuzzi and G. Marrocco, "Constrained-Design of Passive UHF RFID Sensor Antennas," *IEEE Trans. Antennas Propag*., vol. 61, no. 6, pp. 2972 - 2980, June 2013.

[34] SL900A datasheet. [Online]. Available: http://ams.com/eng/Products/UHF-RFID/UHF-Interface-and-Sensor-Tag/SL900A.

0018-926X (c) 2018 IEEE. Personal use is permitted, but republication/redistribution requires IEEE permission. See http://www.ieee.org/publications_standards/publications/rights/index.html for more information.